ACS Chemical Neuroscience

pubs.acs.org/chemneuro Letter

Screening Platform Based on Inductively Coupled Plasma Mass Spectrometry for β-Site Amyloid Protein Cleaving Enzyme 1 (BACE1) Inhibitors

Xin Jin, Limin Yang,* Xiaowen Yan,* and Qiuquan Wang*

Cite This: ACS Chem. Neurosci. 2021, 12, 1093−1099 Read Online

ACCESS | Metrics & More | Article Recommendations | Supporting Information

ABSTRACT: β-Site amyloid protein cleaving enzyme 1 (BACE1) is a promising therapeutic target for developing inhibitors to alleviate Alzheimer's disease (AD). Herein, we established an inductively coupled plasma mass spectrometry (ICPMS)-based inhibitor screening platform. A biotin-labeled lanthanide-coded peptide probe (LCPP; biotin-PEG_2-EVNLDAEC-DOTA-Ln) was designed to determine the activity of BACE1 and evaluate the degree of inhibition of inhibitors. The platform was first validated with two commercially available inhibitors (BSI I and BSI IV) in terms of IC_{50} values and then applied to two newly designed inhibitors (inhibitors II and III) based on the crystal structure of BACE1 interacting with inhibitor I, and each of them contained an acylguanidine core structure. We found that their inhibition effects were improved as evaluated by the sensitive and accurate LCPP−ICPMS platform, demonstrating its ability for new drug screening.

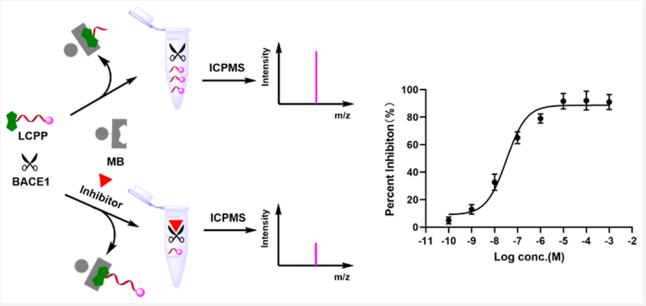

KEYWORDS: *Inductively coupled plasma mass spectrometry (ICPMS), BACE1, BACE1 inhibitor, lanthanide, element-tag*

BACE1, also known as β-site amyloid precursor protein (APP)-cleaving enzyme 1 or β-secretase, is the rate-limiting enzyme that produces toxic peptides Aβ40 and Aβ42, according to the amyloid cascade hypothesis.[1,2] Several studies observed a lower production of Aβ with minor effects on normal physiological processes of mice whose BACE1 gene was knocked out.[3,4] Recent studies revealed that BACE1 levels increased in the cortices and plasma of Alzheimer's disease (AD) patients.[5,6] Therefore, BACE1 is considered as a promising therapeutic target for AD treatment, and a growing number of BACE1 inhibitors with different structures have been constantly reported.[7−12]

The development of a simple, sensitive, and reliable method to detect BACE1 and screen its inhibitors is crucial for clinical diagnosis and treatment of AD. Until now, several methods such as enzyme-linked immunosorbent assay, surface plasmon resonance (SPR), and fluorescence resonance energy transfer (FRET) have been developed for this purpose.[13−16] Among them, FRET is most frequently used one mainly due to its sensitivity and high-throughput capability. However, conventional FRET assay presents shortcomings such as narrow Stokes shifts and spectral overlap of near-UV excitation wavelengths of some fluorophores with the absorption peaks of many small background molecules containing aromatic rings, so the choice of suitable donor/acceptor pairs has to be varied from study to study for their applications.[16−19] Furthermore, the peptide substrates should be carefully optimized to achieve high FRET efficiency, avoiding the frequently encountered steric hindrance and low solubility issues owing to the presence of hydrophobic fluorophores at each end of the peptide substrates.[16,18] Although use of quantum dots and layered tungsten disulfides has been attempted to solve these problems, they could not be used in acid pH medium in which BACE1 exhibits higher activity.[14,16] More seriously, the synthetic and natural inhibitors containing aromatic rings could absorb or quench the light signals, leading to false-positive or false-negative results in some cases.[20,21]

Inductively coupled plasma mass spectrometry (ICPMS) is an ideal technology capable of determining multiple metallic elements simultaneously at ppt level with high accuracy and broad dynamic range.[22] In ICP, a hard ion source, molecules are completely broken down into atomic ions; the signal response is therefore independent of species and matrix.[23,24] Because of these unique features, ICPMS has been applied to the quantification of proteins, DNA, and bacteria as well as

Received: December 24, 2020
Accepted: March 23, 2021
Published: March 25, 2021

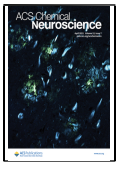

viruses with the aid of diverse element-tagging strategies.[25−33] On the other hand, metal-tagged substrates have also been applied to measure protease activity, demonstrating the advantage of ICPMS compared with the reported optical methods for enzyme assay.[34,35] We previously reported an ICPMS-based multiplex protease assay through Ln-coded protease-specific peptide-nanoparticle probes, during which only a centrifugation step was needed to separate the cleaved probes from the uncleaved ones for ICPMS analysis.[35]

Herein, we established an ICPMS-based inhibitor screening platform enabling not only BACE1 activity assay but also inhibitor screening through a Ln-coded peptide probe (LCPP, Scheme 1A). To start with, we chose EVNLDAE, the Swedish

Scheme 1. (A) Structure of Ln-Coded Peptide Probe (LCPP) and (B) Schematic Illustration of ICPMS-Based BACE1 Assay and Inhibitor Screening Using LCPP

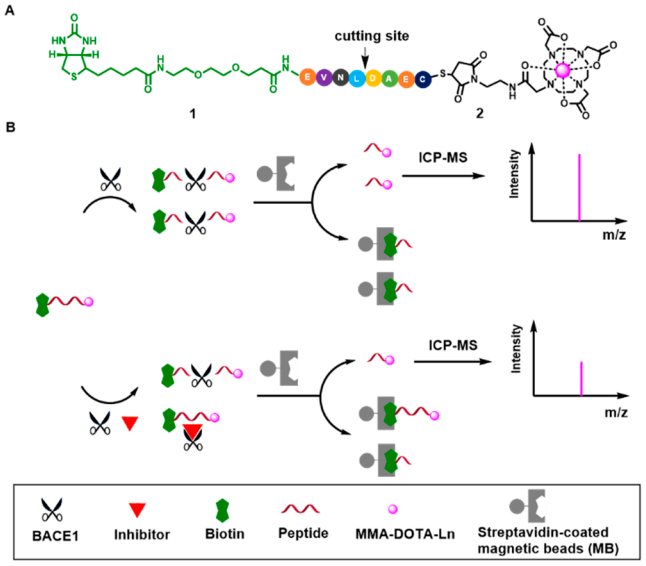

mutated sequence of APP that can be specifically recognized by BACE1 as the substrate.[36] It was further chemically modified to add cysteine (C) to glutamic acid (E) on the C-terminal end, resulting in EVNLDAEC. Afterward, a biotin group was conjugated to the amino group on the N-terminal end using biotin-PEG_2-NHS, the hydrophilic PEG_2 linker of which may improve the solubility of the probe in aqueous solutions. In order to read out element signal in ICPMS, we conjugated lanthanide-loaded 1,4,7,10-tetraazacyclododecane-1,4,7-tris(acetic acid)-10-maleimidoethylacetamide (MMA-DOTA-Ln) to biotin-PEG_2-EVNLDAEC on the cysteine residue based on a Michael addition reaction to obtain LCPP (Scheme S1). Detailed procedures can be found in Methods section and ESI-MS spectra for the synthesized biotin-peptide-MMA-DOTA-Ln (Ln = Eu, La, Pr, Nd) LCPP probes are shown in Figure S1 in the Supporting Information.

When BACE1 meets LCPP, it cleaves LCPP specifically at the peptide bond between leucine (L) and aspartic acid (D), resulting in biotin-EVNL and DAEC-MMA-DOTA-Ln (Scheme 1A). The resulting biotin-EVNL and the remaining uncleaved LCPP can be pulled down using streptavidin-functionalized magnetic beads because of the strong interaction between biotin and streptavidin, while the DAEC-MMA-DOTA-Ln in the supernatant can be subjected to ICPMS quantification via the determination of Ln (Scheme 1B). When a BACE1 inhibitor is present, BACE1 activity is blocked, resulting in reduced LCPP cleavage and therefore the corresponding Ln ICPMS signal decrease (Scheme 1B). The decrease in the ICPMS Ln-signal intensity is correlated with the degree of inhibition of the inhibitor, meaning that stronger inhibitors cause lower Ln-signal on ICPMS. In this way, we are able not only to determine the activity of BACE1 on the LCPP−ICPMS platform but also to assess the inhibition effect of its potential inhibitors, thus effectively screening BACE1 inhibitors.

In order to confirm that BACE1 could hydrolyze LCPP, in a preliminary experiment we incubated 40 nM BACE1 and 10 μM LCPP in sodium acetate buffer and monitored the cleaved products by HPLC-ESI-MS. As shown in Figure 1, LCPP was

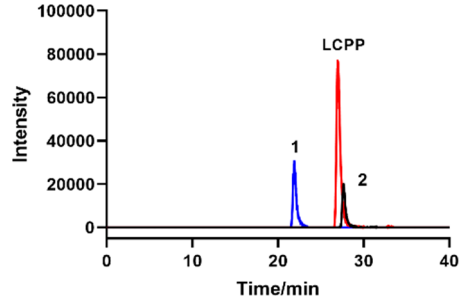

Figure 1. Selected ion chromatograms from HPLC-ESI-MS monitoring the cleaved products of LCPP. LCPP (10 μM, red peak) and BACE1 (40 nM) were first incubated in sodium acetate buffer (20 mM, pH 4.5) at 37 °C for 120 min; the cleaved products were then monitored by HPLC-ESI-MS. Peaks 1 and 2 represent DAEC-MMA-DOTA-Eu (blue peak) and biotin-EVNL (black peak), respectively.

precisely hydrolyzed by BACE1 at the cutting site between L and D. The two cleaved products of DAEC-MMA-DOTA-Eu (peak 1 at 22.0 min) and biotin-EVNL (peak 2 at 27.5 min) were confirmed by ESI-MS (Figure S2), demonstrating the feasibility of our designed probe for BACE1 cleavage.

Next, we optimized the reaction conditions to improve the probe performance. The results obtained from the experiments on time-dependent cleavage of LCPP by BACE1 indicated that the ICPMS signal of BACE1-cleaved DAEC-MMA-DOTA-Eu increased along with the increase in the incubation time from 0 to 60 min, and then gradually reached a plateau after 60 min (Figure S3A). We therefore chose 60 min as the incubation time for the following experiments. The pH value of the reaction buffer has a significant influence on BACE1 activity. BACE1 exerts its enzymatic activity through a general acid−base mechanism, in which Asp228 acts as a base to activate a bridging catalytic water, while Asp32 acts as an acid to protonate the substrate carbonyl group.[37−39] It was reported that BACE1 cleavage occurs in cellular acid compartments, for example, endosomal or trans-Golgi network,[40] so we chose pH values varying from 3.5 to 6.0 to study the pH-dependent BACE1 activity. As shown in Figure S3B, the maximum ^{153}Eu signal was obtained at pH 4.5, which is consistent with the results reported in the literature.[41,42] Previous simulation studies revealed a detailed mechanism of the pH-regulated enzymatic activity. When the catalytic dyad is monoprotonated at pH 4.5, a binding-competent state is highly occupied, which is conducive to substrate binding.[43] We therefore chose 4.5 as the optimal pH in the subsequent experiments.

https://doi.org/10.1021/acschemneuro.0c00816
ACS Chem. Neurosci. 2021, 12, 1093−1099

To further confirm the specificity of LCPP toward BACE1, 1 μM probe was incubated with 20 nM pepsin, trypsin, papain, pectinase, bovine serum albumin (BSA), and BACE1. As depicted in Figure 2A, significant ^{153}Eu signal was determined

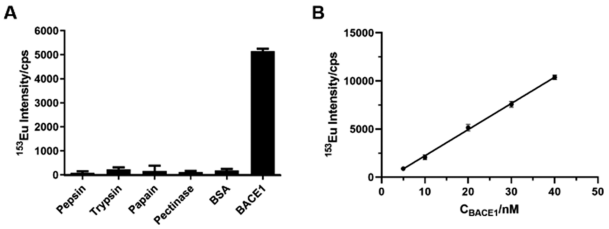

Figure 2. (A) Specificity of LCPP toward BACE1. LCPP was incubated with 20 nM pepsin, trypsin, papain, pectinase, BSA, or BACE1. (B) Linear relationship between ^{153}Eu signals and the concentration of BACE1. Experiments were performed in sodium acetate buffer (20 mM, pH 4.5) containing 1 μM LCPP (n = 3).

only in the presence of BACE1, while other enzymes and proteins produced negligible signals under the same reaction conditions, demonstrating the high specificity of LCPP toward BACE1.

After the LCPP working conditions were optimized, we applied the probe for BACE1 assay. As shown in Figure 2B, with increase of the BACE1 concentration from 4 to 40 nM, a linear increase of ^{153}Eu signal intensity from the cleaved probe was detected by ICPMS. The limit of detection (LOD, 3σ) was calculated to be 0.5 nM BACE1, which is much lower than the results obtained using quantum dot−gold nanoparticle assembly (0.15 μM) and SPR (10 nM) reported in the literature.[14,16] In addition, the LOD obtained from the FITC-labeled probe that we synthesized (Figure S4A) was found to be 22 nM BACE1. The possible reason for the lower sensitivity obtained from the FITC-labeled probe is the lower fluorescence emission of FITC (Figure 4B) at pH 4.5, the optimal pH for BACE1 (Figure S3B).

In order to validate that this probe can be applied to screen BACE1 inhibitors, two commercially available BACE1 inhibitors were selected to evaluate their IC_{50} values. BSI I is a statine-based peptide mimetic inhibitor with an IC_{50} value of 30 nM, while BSI IV is a cell-permeable isophthalamide compound containing a hydroxyethylamine moiety with an IC_{50} value of 29 nM.[7,13] After BACE1 was first treated with different concentrations of BSI I and BSI IV for 30 min, the IC_{50} values were measured on the established LCPP−ICPMS platform and determine to be 32 ± 3 nM for BSI I (Figure 3A, n = 3) and 37 ± 2 nM for BSI IV (Figure 3B, n = 3). These results demonstrated the ability of LCPP−ICPMS to screen BACE1 inhibitors. In addition to the well-known BACE1 inhibitors BSI I and BSI IV, we also chose donepezil, which is an acetylcholinesterase inhibitor, to further validate the LCPP−ICPMS screening platform. No inhibitory effect was observed even when the concentration of donepezil was up to 1 mM (Figures 3C). This is a correct result because donepezil is an inhibitor of acetylcholinesterase but not of BACE1, being consistent with results accessed using unlabeled substrates by CE-MS and MALDI-MS.[44,45] However, an inhibition effect of donepezil in sub-micromolar range toward BACE1 using the FRET substrate was reported.[20,46] These conflicting results might be due to the quenching of fluorophore by donepezil in a concentration-dependent manner.[44−47] Conclusively, our

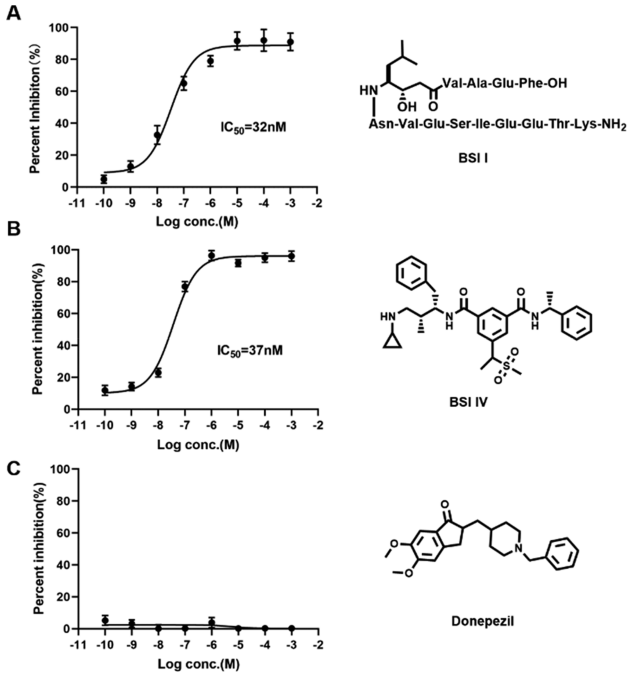

Figure 3. Sigmoidal dose response curves of BACE1 activity versus logarithmic concentration of the compositionally and structurally different BSI I (A), BSI IV (B), and donepezil (C). Experiments were performed in sodium acetate buffer (20 mM, pH 4.5) containing 1 μM LCPP and 20 nM BACE1.

study confirmed that accurate result could be obtained on the established LCPP−ICPMS platform.

Furthermore, on the basis of the crystal structure of BACE1 complexed with acylguanidine-based inhibitor I (IC_{50} = 3.7 μM,[48] Figure 4A, http://www1.rcsb.org/structure/2QU2), we designed two new inhibitors that are expected to have higher inhibitory ability toward BACE1. The acylguanidine moiety of inhibitor I forms four key hydrogen-bonding interactions with the catalytic aspartic acids, Asp32 and Asp228. The two aryl groups (P1, P2′) extend into the S1 and S2′ pockets, respectively, and the para position of the P1 phenyl group projects directly toward the unoccupied S3 pocket, providing an opportunity to add substituents to the P1 phenyl that may extend into the S3 pocket; therefore additional interactions will increase the binding affinity. On the other hand, the S2′ pocket provides access to more polar and charged groups, thus offering the potential to form additional hydrogen bonds directly with BACE1. Moreover, one of the nitrogen groups of the acylguanidine moiety faces away from the catalytic residues toward the S1′ pocket; substitution on this nitrogen might allow access to the unoccupied S1′ pocket, thus presenting potential opportunities to form polar or hydrogen-bonding interactions. Based on these possibilities, inhibitor II was designed by introducing two F atoms on the P2′ phenyl group to facilitate hydrogen bonds with the S2′ pocket (Figure 4C), while inhibitor III was designed by introducing a *para-n*-butoxyphenyl substitution on the P1 phenyl group and a propanol substitution of the acylguanidine moiety to extend into the S3 pocket and S1′ pocket (Figure 4D), respectively. We further replaced the P2′ phenyl with pyrimidine to facilitate a hydrogen bond with the S2′ pocket (Figure 4D). The detailed chemical synthesis and characterization are shown in Scheme S2, Scheme S3 and Figures S5−S18.

https://doi.org/10.1021/acschemneuro.0c00816
ACS Chem. Neurosci. 2021, 12, 1093−1099

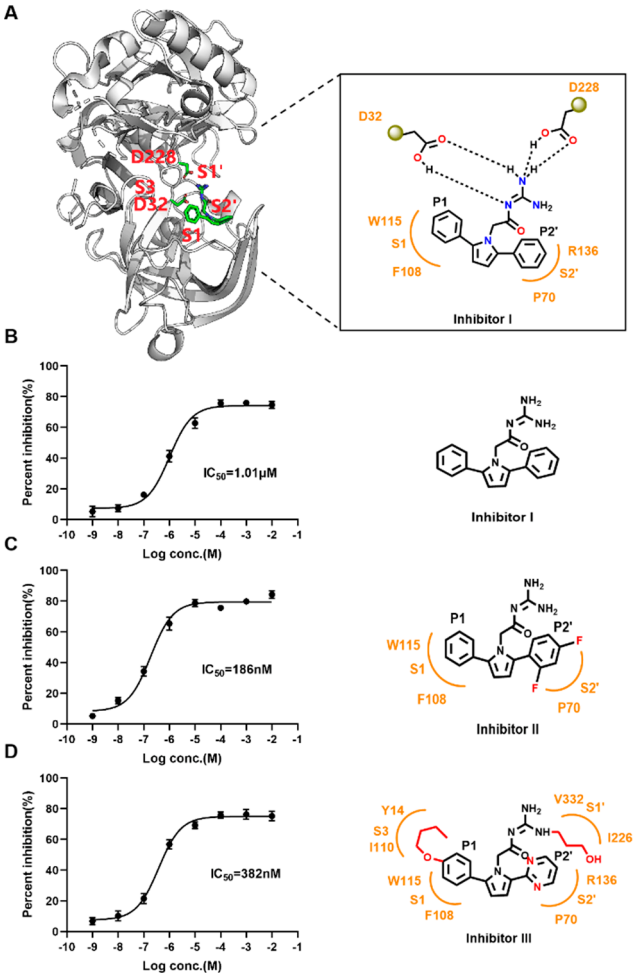

Figure 4. (A) The bonding mode of inhibitor I with BACE1. X-ray crystal structure of inhibitor I binding with BACE1 (PDB code 2QU2, left); the relative locations of the different binding pockets of the active site are labeled, and key amino acid residues and key binding interactions (right) are given. Sigmoidal dose response curves of BACE1 activity versus logarithmic concentration of inhibitor I (B), inhibitor II (C), and inhibitor III (D). Experiments were performed in sodium acetate buffer (20 mM, pH 4.5) containing 1 μM LCPP and 20 nM BACE1.

Considering that ICPMS can easily distinguish and quantify multiple Ln, we encoded LCPP with different Ln ions to measure the IC_{50} values of the newly synthesized BACE1 inhibitors. As shown in Scheme S4, to determine the IC_{50} values of the acylguanidine-based inhibitors using three different Ln-encoded LCPPs (Ln = La, Pr, Nd), the BACE1-cleaved DAEC-MMA-DOTA-Ln in the supernatants were combined and analyzed by ICPMS simultaneously. The determined IC_{50} values of inhibitors I, II, and III were 1.01 $\pm$ 0.25 μM, 186 $\pm$ 2 nM, and 382 $\pm$ 2 nM (n = 3) (Figure 4B–D), suggesting that inhibitor II resulting from the simple introduction of two F atoms on P2′ phenyl group of inhibitor I is more efficacious than inhibitor III with the more complicated structure. Clearly, sophisticated design of BACE1 inhibitory molecules is much more desired in the future, and they can be precisely evaluated on the established LCPP–ICPMS platform.

In summary, we have successfully developed a sensitive and accurate LCPP–ICPMS platform for not only BACE1 assay but also BACE1 inhibitor screening. The LCPP features a peptide substrate of which one end is tagged with a DOTA-Ln that can be encoded with different Ln ions on demand and the other end is labeled with a biotin group enabling the highly efficient separation of the cleaved Ln from uncleaved LCPP for accurate ICPMS quantification. Such a design allows us to screen BACE1 inhibitors via switching the determination of the hydrolyzed polypeptide fragments to quantification of Ln on ICPMS. To the best of our knowledge, this is the first example applying ICPMS for inhibitor screening. This methodology should be very much expected to be applied to the screening of other enzymes inhibitors, not limited to BACE1 demonstrated here.

METHODS

Synthesis of LCPP and FITC-Labeled Probe. Triethylamine (TEA, 4.3 μL, 32.4 μmol) and biotin-NHS ester (8.1 mg, 16.2 μmol) were added into peptide EVNLDAEC (9.6 mg, 10.8 μmol) with anhydrous *N*,*N*-dimethylformamide (DMF, 100 μL) as solvent. After overnight reaction, the mixture was purified using the semipreparative HPLC with a TechMate C18-ST column (10.0 i.d. × 250 mm in length, 5 μm particle size), during which H_2O/ACN mixture was used as the mobile phase with a gradient elution program from 70/30 H_2O/ACN to 20/80 H_2O/ACN in 30 min at a flow rate of 4.0 mL/min, followed by reduced pressure distillation and freeze-drying to give biotin-EVNLDAEC (10.0 mg, yield 72%). Then, the obtained biotin-EVNLDAEC (10.0 mg, 7.82 μmol) and MMA-DOTA-Eu (13.5 mg, 20 μmol) were dissolved in ammonium acetate buffer (0.2 mL, 100 mM, pH 6.4) and stirred for 3 h at 37 °C and then purified by HPLC to obtain biotin-peptide-DOTA-Eu (13.0 mg, yield 85%). Biotin-peptide-MMA-DOTA-Ln (Ln = La, Pr, Nd) were prepared in the same way as biotin-peptide-MMA-DOTA-Eu. (Scheme S1) They were characterized using ESI-MS (Figure S1). The synthetic route for FITC-labeled probe was similar to that for LCPP just using FITC instead of MMA-DOTA-Ln. The obtained biotin-EVNLDAEC (5.0 mg, 3.9 μmol) and MMA-FITC (4.3 mg, 10 μmol) were dissolved in ammonium acetate buffer (0.2 mL, 100 mM, pH 6.4) and stirred for 3 h at 37 °C, then purified by HPLC to obtain FITC-labeled probe (5.0 mg, yield 75%).

Synthesis of 1-(2,4-Difluorophenyl)-4-phenylbutane-1,4-dione (Compound 1). To a solution of $ZnCl_2$ (5.0 g, 36.7 mmol) in toluene (40 mL) was added diethylamine (DEA, 2.9 mL, 27.5 mmol) followed by *t*-BuOH (2.6 mL, 27.5 mmol). The mixture was stirred at room temperature (RT) for 2 h until it was mostly dissolved; then acetophenone (3.3 mL, 27.5 mmol) and 2-bromo-2′,4′-difluoroacetophenone (4.3 g, 18.4 mmol) were added to the reaction mixture for 6 h reaction under stirring, and the reaction mixture was diluted with water (40 mL), extracted with CH_2Cl_2 (3 × 40 mL), dried with $MgSO_4$, and filtered through a funnel in sequence. The filtrate was concentrated in vacuo and purified by silica gel flash column chromatography (EtOAc/petroleum ether (PE), 1/40) to give a yellow powder, compound **1** (2.1 g, yield 42%) (Scheme S2). ^{1}H NMR (500 MHz, $CDCl_3$) δ 8.07–7.99 (m, 2H), 7.96 (td, J = 8.6, 6.7 Hz, 1H), 7.61–7.54 (m, 1H), 7.47 (t, J = 7.7 Hz, 2H), 7.01–6.92 (m, 1H), 6.89 (ddd, J = 11.1, 8.7, 2.5 Hz, 1H), 3.42 (dhept, J = 9.5, 2.8 Hz, 4H). ^{13}C NMR (125 MHz, $CDCl_3$) δ 198.4, 195.3 (d, J = 4.7 Hz), 166.8 (d, J = 12.2 Hz), 164.8 (d, J = 12.4 Hz), 163.9 (d, J = 12.6 Hz), 161.9 (d, J = 12.5 Hz), 136.7, 133.1, 132.7 (dd, J = 10.6, 4.3 Hz), 128.6, 128.1, 122.0 (dd, J = 13.2, 3.6 Hz), 112.2 (dd, J = 21.4, 3.5 Hz), 104.8 (dd, J = 27.7, 25.4 Hz), 37.2 (d, J = 8.4 Hz), 32.5 (d, J = 2.3 Hz). MS calcd for $C_{16}H_{12}F_2O_2$ $[M + H]^+$ m/z 275.0878, found 275.0870.

Synthesis of 2-(2-(2,4-Difluorophenyl)-5-phenyl-1*H*-pyrrol-1-yl) Acetic Acid (Compound 2). A solution of compound **1** (2.1 g, 7.5 mmol) and glycine (1.7 g, 22.5 mmol) in acetic acid (20 mL) was refluxed at 130 °C overnight. The mixture was naturally cooled to RT, diluted with H_2O (20 mL), extracted with EtOAc (3 × 20 mL), dried with $MgSO_4$, and filtered through a funnel in sequence. The filtrate was concentrated in vacuo and purified by silica gel flash column

https://doi.org/10.1021/acschemneuro.0c00816
ACS Chem. Neurosci. 2021, 12, 1093–1099

chromatography (EtOAc/PE/HCOOH, 1/10/0.01) to obtain compound **2** as a white powder (2.3 g, yield 98%) (Scheme S2). ^{1}H NMR (500 MHz, $CDCl_3$) δ 7.42−7.28 (m, 3H), 6.89 (t, J = 8.7 Hz, 1H), 6.33 (d, J = 3.5 Hz, 1H), 6.31 (d, J = 3.6 Hz, 1H). ^{13}C NMR (125 MHz, $CDCl_3$) δ 174.6, 163.9 (d, J = 12.1 Hz), 161.9 (d, J = 12.0 Hz), 161.1 (d, J = 12.2 Hz), 159.1 (d, J = 12.5 Hz), 137.0, 133.5 (dd, J = 9.2, 4.3 Hz), 132.7, 129.2, 128.7, 128.6, 127.7, 117.2−116.5 (m), 111.7 (dd, J = 20.8, 4.1 Hz), 111.2, 109.8, 104.3 (t, J = 25.9 Hz), 46.5 (d, J = 3.1 Hz). MS calcd for $C_{18}H_{13}F_2NO_2$ $[M + H]^+$ m/z 314.0987, found 314.1020.

Synthesis of *N*-(Diaminomethylene)-2-(2-(2,4-difluorophenyl)-5-phenyl-1*H*-pyrrol-1-yl) Acetamide (Inhibitor II). To a solution of compound **2** (2.3 g, 7.4 mmol) in anhydrous DMF (4.0 mL) was added 1,1′-carbonyldiimidazole (CDI, 1.7 g, 10.5 mmol), and the mixture was stirred at RT for 1 h. To the reaction mixture was added a solution of guanidine hydrochloride (2.5 g, 26.1 mmol) and TEA (3.6 mL, 26.1 mmol) in DMF (6.5 mL). After stirring for 6 h, the above mixture was poured into H_2O (10 mL). The aqueous phase was extracted with EtOAc (3 × 10 mL), and the combined organic layers were dried with $MgSO_4$ and then filtered through a funnel. The filtrate was concentrated in vacuo and purified by silica gel flash column chromatography (EtOAc/PE/HCOOH, 2/8/0.01) to obtain inhibitor II (2.6 g, yield 98%) (Scheme S2). ^{1}H NMR (500 MHz, $CDCl_3$) δ 7.88 (d, J = 3.5 Hz, 4H), 7.33−7.27 (m, 4H), 7.25 (ddd, J = 8.6, 5.2, 2.3 Hz, 2H), 6.82 (ddt, J = 16.3, 9.1, 4.6 Hz, 2H), 6.29−6.24 (m, 2H), 4.58 (s, 2H). ^{13}C NMR (125 MHz, $CDCl_3$) δ 172.5, 163.9 (d, J = 12.2 Hz), 161.9 (d, J = 12.2 Hz), 161.1 (d, J = 12.5 Hz), 159.1 (d, J = 12.2 Hz), 156.2, 137.3, 134.0−133.1 (m), 132.6, 129.1, 128.8, 128.7, 127.8, 116.7 (dd, J = 15.0, 4.4 Hz), 111.8 (d, J = 24.5 Hz), 111.5, 110.0, 104.4 (t, J = 25.8 Hz), 49.1. MS calcd for $C_{19}H_{16}F_2N_4O$ $[M + H]^+$ m/z 355.1370, found 355.1365.

Synthesis of 1-(4-Butoxyphenyl)-3-(dimethylamino) Propan-1-one (Compound 3). A solution of 4′-butoxyacetophenone (2.5 g, 13.0 mmol), dimethylamine hydrochloride (DMA, 1.4 g, 14.6 mmol), paraformaldehyde (PA, 0.6 g, 19.7 mmol), and 12 N HCl (25 μL) in ethanol (10 mL) was refluxed at 100 °C overnight. The solution was naturally cooled to RT, and the ethanol was evaporated under vacuum; a 20% aqueous solution of NaOH was added to adjust pH = 10, and then the residue was extracted with EtOAc (3 × 20 mL). The combined organic layers were dried with $MgSO_4$ and filtered through a funnel. The filtrate was concentrated in vacuo and purified by silica gel flash column chromatography (EtOAc/MeOH, 10/1) to give compound **3** (1.6 g, yield 49%) (Scheme S3). ^{1}H NMR (500 MHz, $CDCl_3$) δ 7.93 (d, J = 9.0 Hz, 2H), 6.92 (d, J = 8.9 Hz, 2H), 4.02 (t, J = 6.5 Hz, 2H), 3.10 (dd, J = 8.0, 6.8 Hz, 2H), 2.75 (dd, J = 8.0, 6.8 Hz, 2H), 2.29 (s, 4H), 1.79 (dq, J = 8.2, 6.7 Hz, 2H), 1.55−1.44 (m, 2H), 0.98 (t, J = 7.4 Hz, 3H). ^{13}C NMR (125 MHz, $CDCl_3$) δ 197.6, 163.1, 130.3, 129.8, 114.2, 67.9, 54.6, 45.5, 36.5, 31.1, 19.2, 13.8. MS calcd for $C_{15}H_{23}NO_2$ $[M + H]^+$ m/z 250.1802, found 250.1750.

Synthesis of Pyrimidine-2-carbaldehyde (Compound 4). To a solution of 2-iodoxybenzoic acid (IBX, 7.6 g, 27.3 mmol) in ACN (20 mL) was added 2-pyrimidinemethanol (1.0 g, 9.1 mmol), and the reaction mixture was stirred at 80 °C for 3 h in N_2 atmosphere, then filtered through a funnel and concentrated in vacuo to give crude compound **4** (Scheme S3), which was directly used for next step of synthesis.

Synthesis of 1-(4-Butoxyphenyl)-4-(pyrimidin-2-yl) Butane-1,4-dione (Compound 5). To a well stirred solution of compound **3** (1.6 g, 6.4 mmol) in 1,4-dioxane (10 mL) was added compound **4** (0.8 g, 7.4 mmol), 3-ethyl-5-(2-hydroxyethyl)-4-methylthiazolium bromide (EHMB, 0.5 g, 2.0 mmol), and TEA (5 mL). The reaction mixture was refluxed at 120 °C for 16 h, the solution was naturally cooled to RT and diluted with H_2O (20 mL), then the mixture was extracted with EtOAc (3 × 30 mL). The combined organic layers were dried over anhydrous $MgSO_4$, filtered through a funnel, and concentrated in vacuo. The residue was purified by silica gel flash column chromatography to give compound **5** (1.0 g, yield 50%) (Scheme S3). ^{1}H NMR (500 MHz, DMSO-d_6) δ 8.68 (d, J = 4.9 Hz, 2H), 7.37−7.26 (m, 2H), 7.22−7.12 (m, 2H), 7.06−6.97 (m, 2H), 6.24 (d, J = 3.8 Hz, 1H), 5.15−4.96 (m, 2H), 4.01 (t, J = 6.4 Hz, 2H), 1.79−1.63 (m, 2H), 1.52−1.35 (m, 2H), 0.94 (t, J = 7.4 Hz, 3H). ^{13}C NMR (125 MHz, $CDCl_3$) δ 198.6, 196.8, 163.2, 160.0, 157.7, 130.4, 129.5, 123.0, 114.2, 67.9, 33.1, 32.7, 31.1, 19.2, 13.8. MS calcd for $C_{18}H_{20}N_2O_3$ $[M + H]^+$ m/z 313.1547, found 313.1467.

Synthesis of 2-(2-(4-Butoxyphenyl)-5-(pyrimidin-2-yl)-1*H*-pyrrol-1-yl) Acetic Acid (Compound 6). The synthetic procedure for compound **6** (Scheme S3) was the same as that for compound **2**. ^{1}H NMR (500 MHz, DMSO-d_6) δ 8.68 (d, J = 4.9 Hz, 2H), 7.41−7.24 (m, 2H), 7.22−7.08 (m, 2H), 7.08−6.93 (m, 2H), 6.24 (d, J = 3.8 Hz, 1H), 4.01 (t, J = 6.4 Hz, 2H), 1.76−1.63 (m, 2H), 1.52−1.33 (m, 2H), 0.94 (t, J = 7.4 Hz, 3H). ^{13}C NMR (125 MHz, DMSO-d_6) δ 171.5, 159.9, 159.0, 157.3, 140.4, 131.7, 130.7, 124.6, 117.8, 115.3, 115.1, 109.5, 79.6, 67.7, 49.4, 31.2, 19.2, 14.1. MS calcd for $C_{21}H_{22}N_2O_3$ $[M + H]^+$ m/z 352.1656, found 352.1413.

Synthesis of 1-(3-Hydroxypropyl) Guanidine (Compound 7). Compound **7** (Scheme S3) was prepared according to a published procedure.[45]

Synthesis of (*E*)-*N*-(Amino((3-hydroxypropyl)amino)-methylene)-2-(2-(4-butoxyphenyl)-5-(pyrimidin-2-yl)-1*H*-pyrrol-1-yl) Acetamide (Inhibitor III). Compound **6** (386.0 mg, 1.1 mmol) and CDI (0.9 g, 5.5 mmol) were dissolved in anhydrous DMF (5.0 mL), and the mixture was stirred at RT for 0.5 h. Compound **7** (1.3 g, 11.0 mmol), TEA (1.5 mL, 11.0 mmol), and 4-dimethylaminopyridine (DMAP, 13.4 mg, 0.1 mmol) were added to the reaction mixture, and the mixture was stirred for 12 h at RT. Then the mixture was concentrated in vacuo and purified by silica gel flash column chromatography to obtain inhibitor III (50.0 mg, yield 10.1%) (Scheme S3). ^{1}H NMR (500 MHz, CD_3OD) δ 8.59 (d, J = 4.9 Hz, 1H), 7.35 (d, J = 8.7 Hz, 1H), 7.24 (dd, J = 8.8, 3.7 Hz, 1H), 7.04 (dd, J = 11.5, 6.7 Hz, 1H), 6.96 (t, J = 6.3 Hz, 1H), 6.23 (dd, J = 7.5, 3.9 Hz, 1H), 5.08 (d, J = 12.6 Hz, 1H), 4.01 (t, J = 6.4 Hz, 1H), 3.61 (dt, J = 29.5, 4.2 Hz, 1H), 3.30 (ddd, J = 15.8, 8.4, 4.2 Hz, 2H), 1.82−1.71 (m, 2H), 1.52 (dq, J = 14.8, 7.4 Hz, 1H), 1.29 (d, J = 4.6 Hz, 1H), 1.00 (td, J = 7.4, 2.6 Hz, 2H). ^{13}C NMR (214 MHz, CD_3OD) δ 171.2, 159.6, 159.4, 156.5, 156.5, 141.1, 130.3, 130.3, 124.4, 116.8, 115.1, 114.3, 109.1, 67.4, 67.4, 58.5, 58.3, 48.9, 48.4, 38.2, 31.1, 31.0, 18.9, 12.8. MS calcd for $C_{24}H_{30}N_6O_3$ $[M + H]^+$ m/z 451.2452, found 451.2351.

Measurement of the IC_{50} Values of Inhibitors I, II, and III. The inhibitors at different concentrations were incubated with 20 nM BACE1 in CH_3COONa (20 mM, pH 4.5) containing 0.01% Triton X-100 at 37 °C for 30 min, and then 1 μM LCPP (La for inhibitor I, Pr for inhibitor II, Nd for inhibitor III) was added, and the reaction was incubated at 37 °C for 60 min with gentle shaking (600 rpm). Subsequently, streptavidin magnetic beads and MOPS buffer (100 mm, pH 7.4) were added to the mixture, and it was incubated on a rotary mixer for 15 min and set on the magnet for 3 min for separation of the uncleaved LCPP from the cleaved DAEC-MMA-DOTA-Ln (Ln = La, Pr, Nd). Finally, the supernatants were mixed and diluted with 2% HNO_3 for ICPMS measurement to obtained the inhibitor-mediated BACE1 activity. Sigmoidal dose response curves of the inhibition percentage (%) versus logarithmic concentration of inhibitor I, inhibitor II, and inhibitor III were thus constructed (Figure 4). From the sigmoidal dose response curves, the IC_{50} value was obtained.

■ ASSOCIATED CONTENT

Supporting Information

The Supporting Information is available free of charge at https://pubs.acs.org/doi/10.1021/acschemneuro.0c00816.

Materials and instrumentation, synthetic routes, measurement of the IC_{50} values of inhibitors I, II, and III, ESI-MS of biotin-peptide-MMA-DOTA-Ln (Eu, La, Pr, Nd), ESI-MS of LCPP, DAEC-MMA-DOTA-Eu, and biotin-EVNL, time and pH-dependent BACE1 proteolytic activity, structure of FITC-labeled probe and fluorescence responses from a series of BACE1

https://doi.org/10.1021/acschemneuro.0c00816
ACS Chem. Neurosci. 2021, 12, 1093−1099

concentrations, and ^{1}H and ^{13}C NMR of the synthesized compounds (PDF)

AUTHOR INFORMATION

Corresponding Authors

Limin Yang − *Department of Chemistry and the MOE Key Laboratory of Spectrochemical Analysis & Instrumentation, College of Chemistry and Chemical Engineering, Xiamen University, Xiamen 361005, China*; Email: lmyang@xmu.edu.cn

Xiaowen Yan − *Department of Chemistry and the MOE Key Laboratory of Spectrochemical Analysis & Instrumentation, College of Chemistry and Chemical Engineering, Xiamen University, Xiamen 361005, China*; orcid.org/0000-0001-6608-6044; Email: xwyan@xmu.edu.cn

Qiuquan Wang − *Department of Chemistry and the MOE Key Laboratory of Spectrochemical Analysis & Instrumentation, College of Chemistry and Chemical Engineering, Xiamen University, Xiamen 361005, China*; orcid.org/0000-0002-5166-4048; Email: qqwang@xmu.edu.cn; Fax: +86 592 2187400

Author

Xin Jin − *Department of Chemistry and the MOE Key Laboratory of Spectrochemical Analysis & Instrumentation, College of Chemistry and Chemical Engineering, Xiamen University, Xiamen 361005, China*

Complete contact information is available at: https://pubs.acs.org/10.1021/acschemneuro.0c00816

Author Contributions

X.Y., L.Y., and Q.W. conceived and supervised the research design and details. X.J. carried out the experiments and analyzed the results. The manuscript was first prepared by X.J., L.Y. and X.Y. and then revised by X.Y. and Q.W.

Notes

The authors declare no competing financial interest.

ACKNOWLEDGMENTS

This study was financially supported by the National Natural Science Foundation of China (21535007, 21874112, and 22074127) and the Fundamental Research Funds for the Central Universities (20720200073). We thank the Foundation for Innovative Research Groups of the National Natural Science Foundation of China (21521004) and Program for Changjiang Scholars and Innovative Research Team in University (PCSIRT, IRT13036) for partial financial support.

REFERENCES

(1) Mattson, M. P. (2004) Pathways towards and away from Alzheimer's disease. *Nature 430*, 631−639.

(2) Cai, H., Wang, Y. S., McCarthy, D., Wen, H. J., Borchelt, D. R., Price, D. L., and Wong, P. C. (2001) BACE1 is the major beta-secretase for generation of Abeta peptides by neurons. *Nat. Neurosci. 4*, 233−234.

(3) Luo, Y., Bolon, B., Kahn, S., Bennett, B. D., Babu-Khan, S., Denis, P., Fan, W., Kha, H., Zhang, J. H., Gong, Y. H., et al. (2001) Mice deficient in BACE1, the Alzheimer's β-secretase, have normal phenotype and abolished β-amyloid generation. *Nat. Neurosci. 4*, 231−232.

(4) Nishitomi, K., Sakaguchi, G., Horikoshi, Y., Gray, A. J., Maeda, M., Hirata-Fukae, C., Becker, A. G., Hosono, M., Sakaguchi, I., Minami, S. S., et al. (2006) BACE1 inhibition reduces endogenous Abeta and alters APP processing in wild-type mice. *J. Neurochem. 99*, 1555−1563.

(5) Yang, L. B., Lindholm, K., Yan, R. Q., Citron, M., Xia, W. M., Yang, X. L., Beach, T., Sue, L., Wong, P., Price, D., et al. (2003) Elevated beta-secretase expression and enzymatic activity detected in sporadic Alzheimer disease. *Nat. Med. 9*, 3−4.

(6) Shen, Y., Wang, H. B., Sun, Q. Y., Yao, H. H., Keegan, A. P., Mullan, M., Wilson, J., Lista, S., Leyhe, T., Laske, C., et al. (2018) Increased plasma beta-secretase 1 may predict conversion to Alzheimer's disease dementia in individuals with mild cognitive impairment. *Biol. Psychiatry 83*, 447−455.

(7) Sinha, S., Anderson, J. P., Barbour, R., Basi, G. S., Caccavello, R., Davis, D., Doan, M., Dovey, H. F., Frigon, N., Hong, J., et al. (1999) Purification and cloning of amyloid precursor protein beta-secretase from human brain. *Nature 402*, 537−540.

(8) Hong, L., Koelsch, G., Lin, X. L., Wu, S. L., Terzyan, S., Ghosh, A. K., Zhang, X. C., and Tang, J. (2000) Structure of the protease domain of memapsin 2 (beta-secretase) complexed with inhibitor. *Science 290*, 150−153.

(9) Ghosh, A. K., and Osswald, H. L. (2014) BACE1 (β-secretase) inhibitors for the treatment of Alzheimer's disease. *Chem. Soc. Rev. 43*, 6765−6813.

(10) Das, B., and Yan, R. Q. (2019) A close look at BACE1 inhibitors for Alzheimer's disease treatment. *CNS Drugs 33*, 251−263.

(11) Chen, J., Wang, J., Yin, B., Pang, L., Wang, W., and Zhu, W. (2019) Molecular mechanism of binding selectivity of inhibitors toward BACE1 and BACE2 revealed by multiple short molecular dynamics simulations and free-energy predictions. *ACS Chem. Neurosci. 10*, 4303−4318.

(12) Chen, J., Yin, B., Wang, W., and Sun, H. (2020) Effects of disulfide bonds on binding of inhibitors to β-amyloid cleaving enzyme 1 decoded by multiple replica accelerated molecular dynamics simulations. *ACS Chem. Neurosci. 11*, 1811−1826.

(13) Pietrak, B. L., Crouthamel, M. C., Tugusheva, K., Lineberger, J. E., Xu, M., DiMuzio, J. M., Steele, T., Espeseth, A. S., Stachel, S. J., Coburn, C. A., et al. (2005) Biochemical and cell-based assays for characterization of BACE-1 inhibitors. *Anal. Biochem. 342*, 144−151.

(14) Yi, X. Y., Hao, Y. Q., Xia, N., Wang, J. X., Quintero, M., Li, D., and Zhou, F. M. (2013) Sensitive and continuous screening of inhibitors of β-site amyloid precursor protein cleaving enzyme 1 (BACE1) at single SPR chips. *Anal. Chem. 85*, 3660−3666.

(15) Folk, D. S., Torosian, J. C., Hwang, S., McCafferty, D. G., and Franz, K. J. (2012) Monitoring β-secretase activity in living cells with a membrane-anchored FRET probe. *Angew. Chem., Int. Ed. 51*, 10795−10799.

(16) Choi, Y., Cho, Y., Kim, M., Grailhe, R., and Song, R. (2012) Fluorogenic quantum dot-gold nanoparticle assembly for beta secretase inhibitor screening in live cell. *Anal. Chem. 84*, 8595−8601.

(17) Kennedy, M. E., Wang, W. Y., Song, L. X., Lee, J., Zhang, L. L., Wong, G., Wang, L. Y., and Parker, E. (2003) Measuring human beta-secretase (BACE1) activity using homogeneous time-resolved fluorescence. *Anal. Biochem. 319*, 49−55.

(18) Zuo, X. W., Dai, H. X., Zhang, H. G., Liu, J. J., Ma, S. D., and Chen, X. G. (2018) A peptide-WS_2 nanosheet based biosensing platform for determination of β-secretase and screening of its inhibitors. *Analyst 143*, 4585−4591.

(19) Mancini, F., Naldi, M., Cavrini, V., and Andrisano, V. (2007) Multiwell fluorometric and colorimetric microassays for the evaluation of beta-secretase (BACE-1) inhibitors. *Anal. Bioanal. Chem. 388*, 1175−1183.

(20) Mancini, F., De Simone, A., and Andrisano, V. (2011) Beta-secretase as a target for Alzheimer's disease drug discovery: an overview of in vitro methods for characterization of inhibitors. *Anal. Bioanal. Chem. 400*, 1979−1996.

(21) Łobiński, R., Schaumlöffel, D., and Szpunar, J. (2006) Mass spectrometry in bioinorganic analytical chemistry. *Mass Spectrom. Rev. 25*, 255−289.

(22) Svantesson, E., Pettersson, J., and Markides, K. E. (2002) The use of inorganic elemental standards in the quantification of proteins

and biomolecular compounds by inductively coupled plasma spectrometry. *J. Anal. At. Spectrom. 17*, 491−496.
(23) Xu, M., Yang, L. M., and Wang, Q. Q. (2008) Quantification of selenium-tagged proteins in human plasma using species-unspecific isotope dilution ICP-DRC-qMS coupled on-line with anion exchange chromatography. *J. Anal. At. Spectrom. 23*, 1545−1549.
(24) Guo, Y. F., Xu, M., Yang, L. M., and Wang, Q. Q. (2009) Strategy for absolute quantification of proteins: CH_3Hg^+ labeling integrated molecular and elemental mass spectrometry. *J. Anal. At. Spectrom. 24*, 1184−1187.
(25) Liu, R., Zhang, S. X., Wei, C., Xing, Z., Zhang, S. C., and Zhang, X. R. (2016) Metal stable isotope tagging: renaissance of radioimmunoassay for multiplex and absolute quantification of biomolecules. *Acc. Chem. Res. 49*, 775−783.
(26) Baranov, V. I., Quinn, Z. A., Bandura, D. R., and Tanner, S. D. (2002) The potential for elemental analysis in biotechnology. *J. Anal. At. Spectrom. 17*, 1148−1152.
(27) Prange, A., and Pröfrock, D. (2008) Chemical labels and natural element tags for the quantitative analysis of biomolecules. *J. Anal. At. Spectrom. 23*, 432−459.
(28) Bettmer, J., Montes-Bayón, M., Ruiz-Encinar, J., Fernández-Sánchez, M. L., Fernández de la Campa, M. d. R., and Sanz-Medel, A. (2009) The emerging role of ICP-MS in proteomic analysis. *J. Proteomics 72*, 989−1005.
(29) Luo, Y. C., Yan, X. W., Huang, Y. S., Wen, R. B., Li, Z. X., Yang, L. M., Yang, C. J., and Wang, Q. Q. (2013) ICP-MS-based multiplex and ultrasensitive assay of viruses with lanthanide-coded biospecific tagging and amplification strategies. *Anal. Chem. 85*, 9428−9432.
(30) Yan, X. W., Yang, L. M., and Wang, Q. Q. (2013) Detection and quantification of proteins and cells by use of elemental mass spectrometry: progress and challenges. *Anal. Bioanal. Chem. 405*, 5663−5670.
(31) de Bang, T. C., and Husted, S. (2015) Lanthanide elements as labels for multiplexed and targeted analysis of proteins, DNA and RNA using inductively-coupled plasma mass spectrometry. *TrAC, Trends Anal. Chem. 72*, 45−52.
(32) Calderón-Celis, F., Encinar, J. R., and Sanz-Medel, A. (2018) Standardization approaches in absolute quantitative proteomics with mass spectrometry. *Mass Spectrom. Rev. 37*, 715−737.
(33) Liang, Y., Liu, Q., Zhou, Y., Chen, S., Yang, L. M., Zhu, M., and Wang, Q. Q. (2019) Counting and recognizing single bacterial cells by a lanthanide-encoding inductively coupled plasma mass spectrometric approach. *Anal. Chem. 91*, 8341−8349.
(34) Lathia, U. S., Ornatsky, O., Baranov, V., and Nitz, M. (2011) Multiplexed protease assays using element-tagged substrates. *Anal. Biochem. 408*, 157−159.
(35) Yan, X. W., Yang, L. M., and Wang, Q. Q. (2011) Lanthanide-coded protease-specific peptide-nanoparticle probes for a label-free multiplex protease assay using element mass spectrometry: a proof-of-concept study. *Angew. Chem., Int. Ed. 50*, 5130−5133.
(36) Mullan, M., Crawford, F., Axelman, K., Houlden, H., Lilius, L., Winblad, B., and Lannfelt, L. (1992) A pathogenic mutation for probable Alzheimer's disease in the APP gene at the N-terminus of beta-amyloid. *Nat. Genet. 1*, 345−347.
(37) Barman, A., Schürer, S., and Prabhakar, R. (2011) Computational modeling of substrate specificity and catalysis of the beta-secretase (BACE1) enzyme. *Biochemistry 50*, 4337−4349.
(38) Toulokhonova, L., Metzler, W. J., Witmer, M. R., Copeland, R. A., and Marcinkeviciene, J. (2003) Kinetic studies on β-site amyloid precursor protein-cleaving enzyme (BACE): confirmation of an iso-mechanism. *J. Biol. Chem. 278*, 4582−4589.
(39) Kocak, A., Erol, I., Yildiz, M., and Can, H. (2016) Computational insights into the protonation states of catalytic dyad in BACE1-acyl guanidine based inhibitor complex. *J. Mol. Graphics Modell. 70*, 226−235.
(40) Westmeyer, G. G., Willem, M., Lichtenthaler, S. F., Lurman, G., Multhaup, G., Assfalg-Machleidt, I., Reiss, K., Saftig, P., and Haass, C. (2004) Dimerization of beta-site beta-amyloid precursor protein-cleaving enzyme. *J. Biol. Chem. 279*, 53205−53212.
(41) Vassar, R., Bennett, B. D., Babu-Khan, S., Kahn, S., Mendiaz, E. A., Denis, P., Teplow, D. B., Ross, S., Amarante, P., Loeloff, R., et al. (1999) Beta-secretase cleavage of Alzheimer's amyloid precursor protein by the transmembrane aspartic protease BACE. *Science 286*, 735−741.
(42) Grüninger-Leitch, P. F., Schlatter, D., Küng, E., Nelböck, P., and Döbeli, H. (2002) Substrate and inhibitor profile of BACE (beta-secretase) and comparison with other mammalian aspartic proteases. *J. Biol. Chem. 277*, 4687−4693.
(43) Ellis, C. R., and Shen, J. (2015) pH-dependent population shift regulates BACE1 activity and inhibition. *J. Am. Chem. Soc. 137*, 9543−9546.
(44) Schejbal, J., Slezáčková, L., Řemínek, R., and Glatz, Z. (2017) A capillary electrophoresis-mass spectrometry based method for the screening of β-secretase inhibitors as potential Alzheimer's disease therapeutics. *J. Chromatogr. A 1487*, 235−241.
(45) Liu, R. F., Liu, Y. C., Meng, J. W., Zhu, H. Y., and Zhang, X. H. (2017) A microfluidics-based mobility shift assay to identify new inhibitors of β-secretase for Alzheimer's disease. *Anal. Bioanal. Chem. 409*, 6635−6642.
(46) Viayna, E., Gomez, T., Galdeano, C., Ramirez, L., Ratia, M., Badia, A., Clos, M. V., Verdaguer, E., Junyent, F., Camins, A., et al. (2010) Novel huprine derivatives with inhibitory activity toward β-amyloid aggregation and formation as disease-modifying anti-Alzheimer drug candidates. *ChemMedChem 5*, 1855−1870.
(47) Shoichet, B. K. (2006) Interpreting steep dose-response curves in early inhibitor discovery. *J. Med. Chem. 49*, 7274−7277.
(48) Cole, D. C., Manas, E. S., Stock, J. R., Condon, J. S., Jennings, L. D., Aulabaugh, A., Chopra, R., Cowling, R., Ellingboe, J. W., Fan, K. Y., et al. (2006) Acylguanidines as small-molecule beta-secretase inhibitors. *J. Med. Chem. 49*, 6158−6161.

https://doi.org/10.1021/acschemneuro.0c00816
ACS Chem. Neurosci. 2021, 12, 1093−1099